Numerical Investigation of Swirl Flow in Curved Tube with Various Curvature Ratio

Aidar Kadyirov[1]
[1]Research Center for Power Engineering Problems of the Russia Academy of Sciences
* Lobachevsky St 2/31, Kazan, Russia, 420111.

Abstract:
Curved tubes are frequently used in many engineering applications [1]. The influences of curvature effects and swirl intensities for Sodium Carboxymethyl cellulose (0.65% NaCMC) flow in a curved tube have been numerically investigated by using COMSOL Multiphysics.

Keywords: curved tube, swirl flow, vortex.

1. Introduction

In the paper [2] by way of example of atmospheric cyclone it is shown that due to the high flow resistance the swirling flow in curved part of the tube is more energy efficient and realizes spontaneously in real-life environment. In this paper we investigate the influence of one of the ways of the forced swirling flow over a steeply curved channels.

2. Use of COMSOL Multiphysics

The mathematical model is developed taking into account a negligibly small gravity force. The steady three-dimensional Navier-Stokes equations are used as the governing equations. Boundary conditions: in the inlet region of the channel velocity field is fully developed, in the outlet region of the channel normal stress is given (the total stress on the boundary is set equal to a stress vector of magnitude, f0=0, oriented in the opposite normal direction). The no-slip condition is forced on the channel walls. To describe the viscosity behavior is taken the Kutateladze model, which based on the structural theory of viscosity and its parameters have physical meaning.
Figure 1 shows the geometric area of the curved channel with insert. Inner diameter of the channel D = 0,05 (m). The twisted tape, which are located directly in front of the curved part, are used as swirl flow generators. The tape is twisted until it reaches an angle of 90 degrees and turns right (fig. 1). The twisted tape is made of sheet metal of thickness 0.002 (m). To avoid the influence of input and output effects the insert is spaced from the entrance to a curved portion L1 = 0,075 (m), where L2 = 0,05 (m).

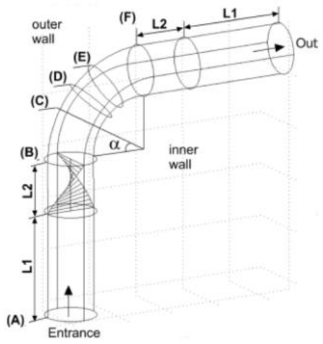

Figure 1. Geometric objects, (A), (B), (D), (F) – crosssections, where (C) – 30º cross-section, (D) – 45º cross-section, (E) – 60º cross-section.

The three-dimensional incompressible Navier-Stokes equations are solved using COMSOL Multiphysics. To solve linear system equations we used "Direct (PARDISO)".
Testing method of solution discussed using the example of laminar flow in a circular tube, bent at an angle of 90 degrees [3] (fig. 2, 3). Good fitness between the numerical and experimental results is received, the error does not exceed 10% .

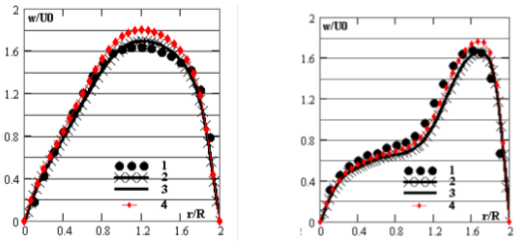

Figure 2. Velocity profile in the central cross-sectional of curved tube: 1 – experiment [4], 2 – FLUENT [3], 3 – SigmaFlow [3], 4 – Comsol Multiphysics; a) – 30° cross-section, b) – 60° cross-section,

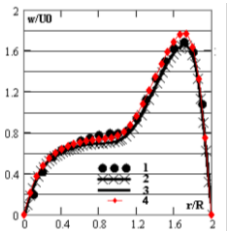

Figure 3. Velocity profile in the central cross-sectional of curved tube: 1 – experiment [4], 2 – FLUENT [3], 3 – SigmaFlow [3], 4 – Comsol Multiphysics; 75° cross-section.

3. Numerical Results

It is known that the availability of the insert as a twisted tape in a straight channel leads to the main flow separates into two parts which rotate relative to each other [5]. The length of the decay of rotating (tangential component of velocity vector is not equal to zero) depends of a few factors including a geometrical shape and a fluid rate.

A similar pattern is observed in the bend (fig.4) where flow twisting device is situated upstream immediately before the bent portion. In the fig.4 U0 - mean velocity; w – actual velocity vector. With increasing radius of bend increasing length of bend, so for R = 1,2 D flux twist does not decay almost the entire length of the curved portion unlike the case where R = 2,5 D.

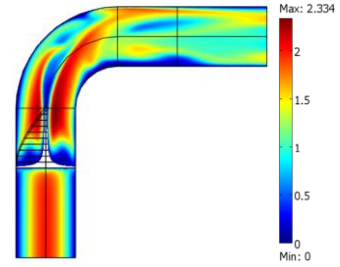

Fig. 4 a)

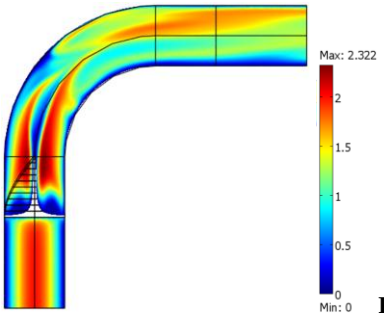

Fig. 4 b)

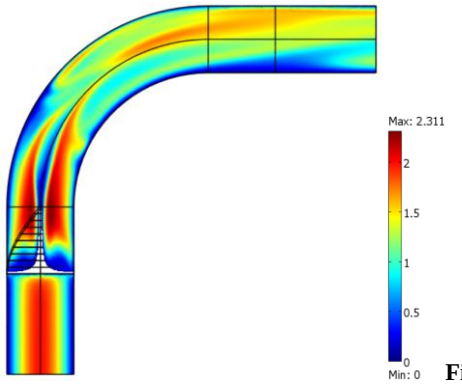

Fig. 4 c)

Figure 4. The relative velocity (U_ns/U0) profile in longitudinal channel section; Re=640; U0 – initial avarege velocity; a) R=1.2D; b) R=2D; c) R=2.5D

To study in detail the influence of twist flux on the fluid flow in a bend velocity profiles in the cross-section of bends for different radiuses were analyzed. In the fig.5 the distributions of relative velocity in the cross-section of bends, having the most interest, are presented.

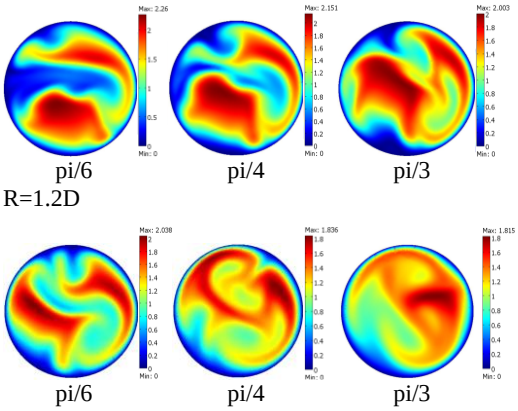

Figure 5 The relative velocity (U_ns/U0) distribution for different cross-section (pi/6, pi/4, pi/3) and curvature ratio (R), Re=640.14, U0 - initial avarege velocity

Development of the flow is the following picture. The swirling flow, getting into the curved portion forms two complex vortexes with different sizes: the largest is located on the inside of the curved channel. Then, these vortexes carried away to the outside of the curved channel due to the inertial forces occurring in the curved pipe. Unlike Dean vortixes considered vortixes

have non-zero radial component of the velocity vector. As the distance increases from the entrance to a curved portion vortixes deform. Therefore, swirl situated on the inside of the bend carry away to outer side, but a small vortex, located on the outer side - to the inside of the bend, all the movements occur in a spiral. Further, downstream with decreasing rate of twist the both vortices damped. As seen from Fig. 5, the damping two vortices ceteris paribus for any curvature radius occurs at different sectors, if, for example, R=1,2 D damping occurs when rotated pi/4, then R = 2,5 D - at pi/3.

Using a twist insert leads to an increase in the energy losses that occur in the flow of fluid in a curved channel, shown in Fig. 1. To quantify account energy losses we use the local coefficient of resistance $\varsigma_{(loc.res.)}$ (1), since in the concerned section the flow rate varies in both magnitude and direction.

$$\varsigma_{(loc.res.)} = \frac{2\Delta p}{\rho U^2} \qquad (1)$$

Where Δp – pressure drop on the concerned section; ρ - fluid density; U - average velocity

The results of numerical studies show (Fig. 6) that at low Reynolds numbers, the greatest energy losses occur as a result of overcoming fluid friction forces concentrated on the channel walls.

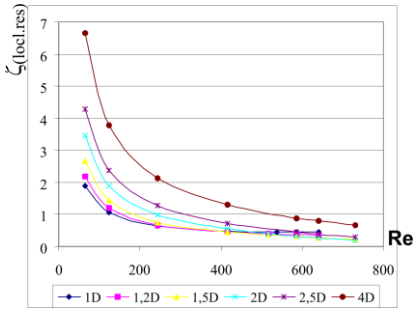

Figure 6 Reynolds-number-dependence of the local resistance in the area between the sections (B) and (F) for different the radius of curvature ratio; R=(1D,…,4D)

Consequently, the value $\varsigma_{(loc.res.)}$ is greatest for the curved channel with a large radius of curvature as the length of its generatrix more than others. Then, with increasing liquid flow rate energy losses resulting from the restructuring of the velocity profile, begin to prevail over the energy losses associated with overcoming the friction forces in the near-wall region, therefore, the value $\varsigma_{(loc.res.)}$ is more for steeply curved channels. It can be seen that, for example, $\varsigma_{(loc.res.)}$ (R=1.2D)< $\varsigma_{(loc.res.)}$ (R=2.5D) at Re <740, and for large Reynolds numbers is observed $\varsigma_{(loc.res.)}$ (R=1.2D)> $\varsigma_{(loc.res.)}$ (R=2.5D). Figure 7 shows Reynolds-number-dependence of the local resistance coefficient in the two areas ((B) - (F), (A) - (F)) for different radius of bend curvature (R = 1D ... 4D).

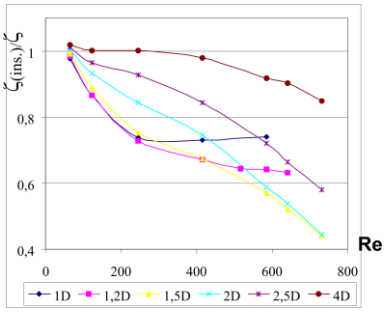

Fig. 7 a)

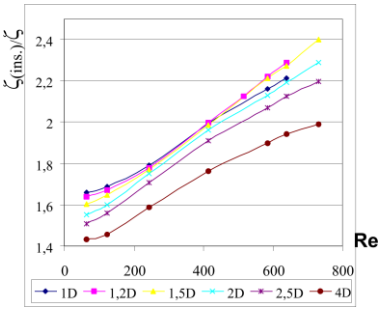

Fig. 7 b)

Figure7. Reynolds-number-dependence of the local resistance for various radius of the bend curvature (R = 1D ... 4D); a) the area between the sections (B) and (F), b) the area between the sections (A) and (F).

In the figure 7(a) ς_{ins} denotes the coefficient of local resistance in the area between sections (B) and (F) with twist tape, ς - the coefficient of local resistance in the area between sections (B) and (F) without twist insert. In the figure 7(b)

ς_{ins} denotes the coefficient of local resistance in the area between sections (A) and (F) with twist insert, ς - the coefficient of local resistance in the area between sections (A) and (F) without twist insert.

It is seen that for low Reynolds numbers, the local coefficient of resistance in the area between sections (B) and (F) for the swirling flow is less than a case when the insert is not used. However, with flow rate increasing the coefficient of the relative local resistance ($\varsigma_{ins}/\varsigma$) starts to increase. As shown by numerical results the trend from decreasing to increasing values of $\varsigma_{ins}/\varsigma$ depends on the radius of the bend and on the flow rate: with increasing radius of the bend the point of local extremum in the plot of (Re) occurs at a higher flow rate. Figure 7 (b) shows Reynolds-number-dependence of $\varsigma_{ins}/\varsigma$ showing the total energy loss of the twisted-tape and the bend. It is seen that the bend R=1,5 D value $\varsigma_{ins}/\varsigma$ substantially coincides with the corresponding value for the bend R = 2D.

4. Conclusions

As a result of the numerical investigations of the influence of the swirling flux on the flow structure and the hydraulic resistance in the curved channel it was obtained the following:
Getting into the curved portion the swirling flow forms two complex vortices with different sizes: the greatest one is on the inner side of the curved channel. Then, these vortices are carried away to the outside of the curved channel due to inertial forces occurring in the curved pipe. Further, with increasing distance from the entrance to the curved portion vortices are deformed and die out;
Transition from a decrease to an increase of the relative coefficient of local resistance in the curved channel was found out. It depends on the radius of the bend and on the flow rate: with increasing radius of the bend the point of an local extremum in the plot of $\varsigma_{ins}/\varsigma$ (Re) occurs at a higher flow rate.

5. References

1. Paisarn Naphon, A review of flow and heat transfer characteristics in curved tubes, *Renewable&Sustainable energy reviews*, **10**, 463-490 (2006)
2. Mingaleeva G.R. Movement of the fluid and gas flow in areas steep spiral rotation path, *Technical Physics Letters*, **28**, 79-84, (2002)
3. Platonov D.V. Platonov D.V., Minakov A.V. Comparative analysis of CFD SigmaFlow and Fluent packages by the example of solving laminar test problems, *Vestnik. Tomsk. State. Univ. Mat. and Mech.*, **1**, 84–94, (2013)
4. Enayet M.M., Gibson M.M. Laser Doppler measurements of laminar and turbulent flow in pipe bend, *NASA contractor report*, **3551**, (1982)
5. Mitrofanova O. V. Fluid dynamics and heat transfer of swirling flows in the channels of the nuclear-electric plants, **286**, (2010)
8. Kadyyrov A.I. The numerical investigation of laminar flow of heat transfer agent in a curved channel with insert, *Izvestiya VUZ. Energy problems*, **9-10**, 78-85, (2012)

6. Acknowledgements

The reported study was supported by RFBR, research project No. 12-08-31067 mol_a